

# ZnOS+C adsorbent for the effective removal of Fast Green dye from synthetic and real wastewater

Sachin<sup>1,2,3</sup>, Biplob Kumar Pramanik<sup>3</sup>, Harshit Gupta<sup>1,2</sup>, Shrawan Kumar<sup>1,2</sup>, Jai Shankar Tawale<sup>1</sup>, Kalpit Shah<sup>3</sup>, Nahar Singh<sup>1,2\*</sup>

<sup>1</sup>BND Division, CSIR-National Physical Laboratory, Dr. K.S. Krishnan Marg, New Delhi-110012, India

<sup>2</sup>Academy of Scientific and Innovative Research (AcSIR), Ghaziabad-201002, India

<sup>3</sup>School of Engineering, RMIT University, Melbourne, VIC 3000, Australia

\*Corresponding author: CSIR-National Physical Laboratory, Dr. K.S. Krishnan Marg, New Delhi 110012, India; E-mail address: naharsingh@nplindia.org (Nahar Singh); Telephone: +91-11-45609221; Fax: +91-11-45609310

## Abstract

Wastewater treatment is becoming increasingly important due to the potential shortage of pure drinking water in many parts of the world. Adsorption offers a potential technique for the uptake of contaminants and wastewater purification. In the last two decades, several efforts have been made to remove fast green (FG) dye from wastewater via different adsorbent materials. But adsorption capacity shown by these adsorbents is low and is time-consuming. Herein, we have synthesized for the first time a new powdered adsorbent ZnOS+C, modified Zinc peroxide with sulfur and activated carbon to effectively remove FG dye from wastewater. Results of batch adsorption experiments have suggested that ZnOS+C has the maximum adsorption capacity of 238.28 mg/g for FG dye within 120 minutes of adsorption equilibrium for a wide range of pH ranging from 2-10 pH. The adsorption process follows the Freundlich isotherm model, suggesting a multilayered adsorption process that occurs on the surface of ZnOS+C. The adsorption kinetics study indicates that the kinetics of the reaction is the intraparticle diffusion model. Briefly, this study shows the proof of application of ZnOS+C powder as a new eco-friendly adsorbent with extremely high efficiency and high surface area for removing FG dye.

**Keywords** ZnOS+C; adsorption; fast green dye; industrial waste; wastewater.

## 1. Introduction

Industrial and municipal wastewater disposal without proper treatment into the environment causes contamination of pure water resources, which further leads to a number of health and environmental problems[1]. The contaminants present in the wastewater may include synthetic dyes[2], heavy metals[3], pesticides[4], pharmaceuticals[5], phenolic species[6], and veterinary products[7]. The wastewater produced from textile industries contains a variety of dyes. Most common and polluting synthetic dyes include fast green, crystal violet, congo red, tartrazine, rhodamine B, and methylene blue. Even their low concentration in water makes them unfit for their use and causes threats to humans[8] and aquatic life[9]. China and India are the major dye manufacturing and exporting countries of dyes[10]. They also have major textile industries. There

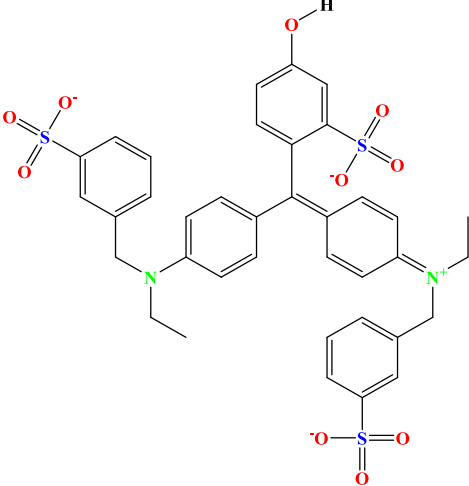
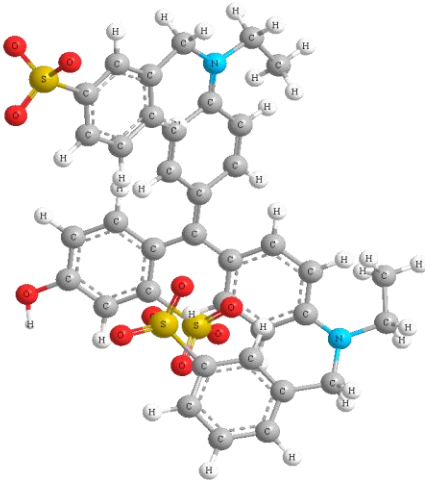
are around 40,000 types of dyes present in the market[11]. The average textile industry uses 10,000 individual dyes for printing and dyeing, consuming a million gallons of water daily[12]. Fast green (FG) dye is widely used in dyeing, textile, food, and household[13]. It is an anionic dye and renders intense green colours[14]. Because of its widespread and careless usage, it leads to contamination of water bodies imparting a green tint, making them improper for consumption and daily usage[15]. Today, almost every country in the world is struggling with the pure water crisis. India, with a population of around 1.3 billion, is significantly affected. The condition in some states of India, such as Maharashtra and Gujrat, is very challenging, and it is an arduous task to supply colorless water. To clean such water requires a lot of time, money, and effort. Therefore, developing an inexpensive and effective technique to decolorize and decontaminate the water is the need of the hour.

Various techniques have been used to remove dyes from wastewater. The techniques are membrane processes, ion exchange method, precipitation, solvent extraction, electrodialysis, reverse osmosis, and adsorption. Every reported technique has some limitations. For example, fouling is a significant problem for the membrane processes[16]. In the ion-exchange approach, regeneration of chemical species is very difficult, and it results in a high cost[17]. The precipitation process generates a lot of sludges, and thus, the management of sludge is an issue[18]. The solvent extraction process requires lots of chemicals and develops a high level of secondary pollution[19]. High power consumption is a significant problem for the electrodialysis process, which makes it not very suitable for dye removal from wastewater.[20]. Out of these processes, the adsorption technique has been found to be the most ideal for the removal of dyes from wastewater. This is because of its essential attributes such as easy to prepare, cheap and good removal, and regeneration efficiency[21].

Several studies have shown to remove dyes from wastewater by natural[22] or synthetic adsorbents[4]. Natural adsorbents are eco-friendly and readily available but have less adsorption capacity[23]. On the other hand, synthetic adsorbent such as activated carbon is conventional and shows good adsorption capacity but has high cost and less selectivity[24]. However, almost all the reported adsorbents have shown an adsorption capacity of less than 100 mg/g for FG dye. For fast green (FG) dye, peanut hull has an adsorption capacity of 15.6 mg/g[25], tur dal husk has 100.39 mg/g[26], tamarind husk adsorbs 101.58 mg/g[26], bottom ash can adsorb up to 20.26 mg/g[27], de-oiled soya adsorbs 5.31 mg/g[27], montmorillonite clay adsorbs 33.45 mg/g[28], and adsorption capacity of 7.56 mg/g is shown by red mud[29]. These adsorbents show a physical adsorption process, which accounts for their low adsorption capacity. However, tur dal husk and tamarind husk have higher adsorption capacity which can be explained on the basis of higher carbon content in them. There is a constant need to improve adsorption capacity to make adsorption processes techno-commercially viable. Zinc peroxide, which has shown the good adsorbent properties for removal of inorganic and organic contaminants from wastewater was initially considered as the potential adsorbent for the FG dye. In this regard, this study focuses on enhancing the adsorption capacity of Zinc peroxide for FG dye by functionalization with sulfur and carbon, synthesizing a new powdered adsorbent ZnOS+C. The functionalization of zinc peroxide with sulfur and carbon is expected to enhance its adsorption properties by making zinc peroxide active for FG dye. This will result in better chemical interactions between adsorbent and the dye and result in better adsorption capacity.

Therefore, the main objectives of this study were (i) the development of a novel ZnOS+C adsorbent by wet chemical route for effective removal of FG dye from real wastewater; (ii) investigation of isotherm and kinetic studies involved, and (iii) elucidate the mechanism involved in adsorption of dye. An approach is made through the advanced characterization method for a better understanding of developed adsorbent and adsorption methods. Several advanced techniques such as X-ray diffraction (XRD), scanning electron microscopy (SEM), energy dispersive x-ray spectroscopy (EDS), and zeta potential was used to understand the properties and adsorption process of the newly developed adsorbent.

**Table 1 Details of Fast Green (FG) dye.**

Fast Green dye	3D structure	Molecular weight (g/mol)
<p><math>C_{37}H_{34}N_2Na_2O_{10}S_3</math></p>  <p>The chemical structure of Fast Green dye is a complex organic molecule. It features a central benzene ring with a hydroxyl group (-OH) at the top position. This central ring is connected to three other benzene rings. One of these rings has a sulfonate group (-SO<sub>3</sub><sup>-</sup>) at the para position. Another ring has a diethylamino group (-N<sup>+</sup>(C<sub>2</sub>H<sub>5</sub>)<sub>2</sub>) at the para position. The third ring is also connected to a fourth benzene ring, which has a sulfonate group (-SO<sub>3</sub><sup>-</sup>) at the para position. The overall structure is highly conjugated and contains multiple sulfonate and diethylamino groups.</p>	 <p>The 3D ball-and-stick model of the Fast Green dye molecule shows the spatial arrangement of atoms. Carbon atoms are represented by grey spheres, hydrogen by white, oxygen by red, sulfur by yellow, and nitrogen by blue. The model illustrates the complex, multi-ring structure and the orientation of the sulfonate and diethylamino groups in three-dimensional space.</p>	808.86

## 2. Experimental section

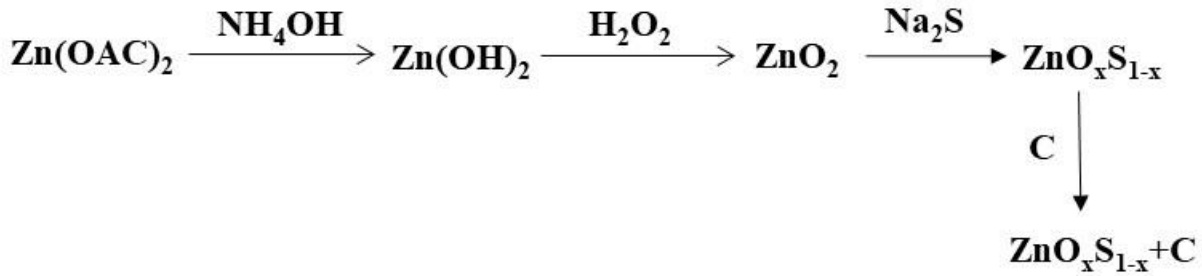
### 2.1. Chemicals

Synthetic wastewater was prepared to conduct the adsorption experiments. For that, de-ionized (DI) water was used with a resistivity of 18.2 MΩ-cm Millipore Milli-Q element water purification system USA. Fast green dye was obtained from CDH, India. Zinc acetate and activated carbon were purchased from Merck, India. Molychem, India supplied sodium sulfide.

### 2.2. Synthesis of ZnOS+C powder

Zinc acetate (100.0 g) was dissolved in water (200 ml), and then ammonium hydroxide was added to the above solution till it became transparent. After that, activated carbon (25.0 g) was added, and the mixture was dried at 70°C for 1 hour, and then hydrogen peroxide (150 ml) was added to the above mixture. At last, sodium sulfide (25.0 g) was added to the above mix, and the precipitate

formed was filtered out using 0.45  $\mu\text{m}$  (filter paper no. 42). The residue was washed several times using DI water prior to drying. The systematic synthesis process is shown below.



### 2.3. Adsorption experiments

A stock solution of 1000 mg/L of FG dye was prepared in DI water. This stock solution was diluted to the desired concentration for batch adsorption studies. Batch adsorption experiments were performed to understand the adsorption capacity of ZnOS+C powder for FG dye. These experiments are performed at room temperature ( $25 \pm 10$  °C). The effect of several adsorption parameters, including adsorbent dosage (10 - 24 mg/25 ml), pH (2 - 10), contact time (30 - 120 min.), and initial concentration of dye (50 - 250 mg/L) was used to conduct the adsorption test. For the adsorption kinetic experiment, adsorbent dosages (10 - 24 mg/25 ml) were added to 250 ml FG dye solution (50 mg/L, 2 pH). The solutions were shaken for 30 to 120 minutes. The samples were collected, and concentrations of samples were analyzed using a UV-VIS spectrometer (624 nm).

The removal of FG dye from wastewater and dye adsorption capacity was calculated using the following equations.

$$\% \text{ Removal of dye} = \frac{C_i - C_f}{C_i} \times 100 \quad (1)$$

$$q_e = \frac{C_i - C_e}{m} \times V \quad (2)$$

Where  $C_i$  and  $C_f$  (mg/L) are the initial and final concentrations of FG dye, respectively,  $C_e$  (mg/L) is the dye concentration at equilibrium conditions.  $q_e$  is the adsorbent capacity of the adsorbent,  $m$  is the mass of adsorbent (g), and  $V$  is the volume of dye solution (L).

The minimum contact time for adsorbent to reach adsorption equilibrium and optimum adsorbent dosage was obtained from the kinetic experiment curves. The controlled experiments were performed using 22 mg/25 ml of adsorbent dosage to study the effect of pH of dye solution and initial dye concentration on the removal efficiency of dye. The adsorption behavior model and maximum adsorption capacity of ZnOS+C adsorbent were determined by adsorption studies using different initial dye concentration studies ranging from 50 to 250 mg/L.

### 2.4. Characterizations

A Fourier transform infrared spectrometer (FT-IR) was used to identify the functional groups present in the ZnOS+C adsorbent. For this, moist free KBR pellets of adsorbent are prepared and scanned in the range of  $4000\text{ cm}^{-1}$  to  $400\text{ cm}^{-1}$  IR band. Powdered X-Ray Diffraction (XRD) analysis of ZnOS+C adsorbent was performed in the 2-theta range of  $20^\circ$  to  $80^\circ$ . Scanning electron microscopy and energy-dispersive X-ray spectroscopy (SEM-EDS) were used to determine the surface morphology and elemental analysis of the ZnOS+C adsorbent before and after the adsorption. The concentration of FG dye in the wastewater samples before and after the adsorption was determined by UV-VIS spectrometer (Hitachi U-3900H). The surface area of synthesized ZnOS+C was analyzed using Brunauer-Emmett-Teller (BET). For zeta potential analysis, pH was varied from 2 to 9 with the help of NaOH and HCL, zeta potential was measured at each pH.

### **3. Result and Discussion**

#### **3.1. Characterizations**

Fourier transform infrared spectra of the ZnOS+C adsorbent is shown in Figure 1 to describe the functional group present in the adsorbent. The peaks at  $429\text{ cm}^{-1}$  and  $460\text{ cm}^{-1}$  are of Zn-O stretching. The transmission peak at  $690\text{ cm}^{-1}$  is due to the O-S stretching bond. The peak at  $1640\text{ cm}^{-1}$  and  $3400\text{ cm}^{-1}$  are of carbon and O-H stretching. No extra peaks in FTIR spectra are observed. X-Ray Diffraction (XRD) is a crystallographic technique used to determine a particular crystal's atomic and molecular structure. Figure 2 shows the obtained XRD spectrum of ZnOS+C powder. The peaks around  $26^\circ$  is of carbon. Other peaks at  $29^\circ$ ,  $32^\circ$ ,  $34^\circ$ ,  $37^\circ$ ,  $42^\circ$ ,  $49^\circ$ ,  $58^\circ$ , and  $69^\circ$  are the corresponding peak of ZnOS[30]. This shows that the ZnOS+C adsorbent is synthesized properly and explains its quality. The adsorbent shape becomes smoother and larger in size after adsorption compared to the shape and size before adsorption as shown in Figure 3(a) and 3(b); this suggests that dye is accumulated on the surface of the adsorbent, and adsorption has taken place. Similarly, Figures 3(c) and 3(d) shows the EDS data of adsorbent before and after adsorption of dye. Some amount of nitrogen is present in Figure 3(d), which cannot be seen earlier in figure 3(c). This suggests that the adsorbent initially doesn't have nitrogen, and it comes from the FG dye adsorbed.

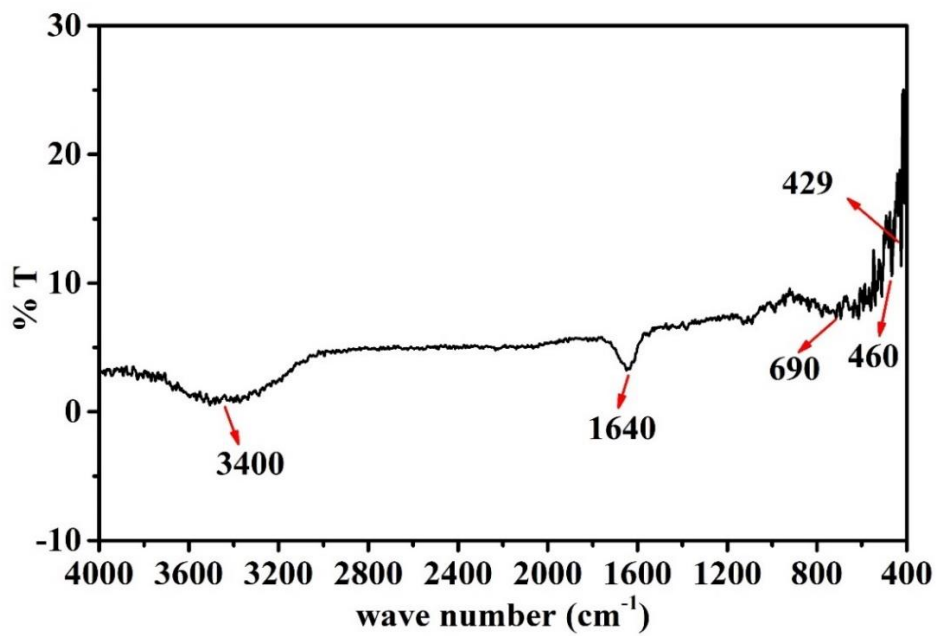


Figure 1 FTIR spectra of ZnOS+C adsorbent.

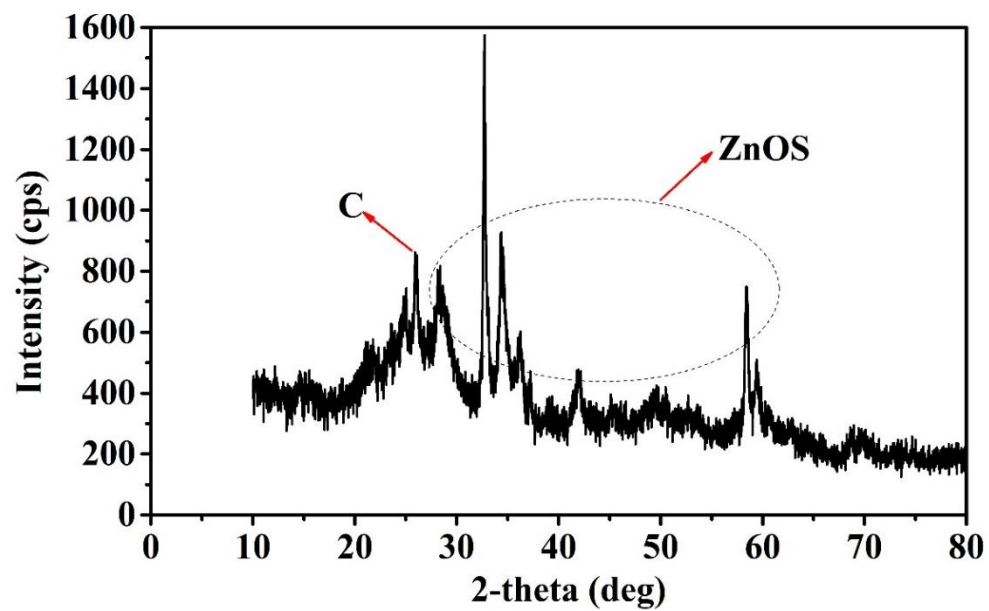
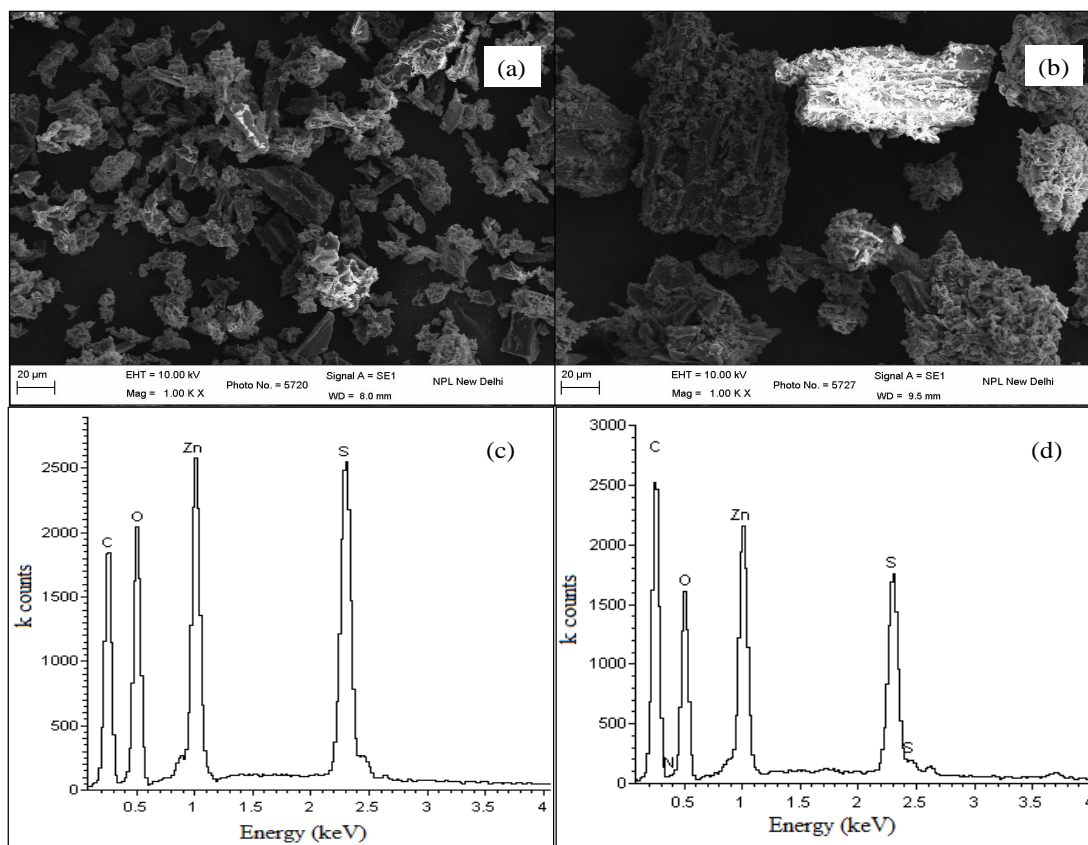


Figure 2 XRD spectra of ZnOS+C adsorbent.



**Figure 3 SEM of (a) ZnOS+C before adsorption, (b) ZnOS+C after adsorption of FG dye, (c) EDS of ZnOS+C before adsorption, (d) EDS of ZnOS+C after adsorption of FG dye.**

The surface area of ZnOS+C was analyzed using a Quantachrome Autosorbic surface analyzer by nitrogen adsorption-desorption curve. With the help of the BET equation surface area of ZnOS+C was found to be  $257.850 \text{ m}^2/\text{g}$ . The surface area is higher as compared to other reported adsorbents, and the higher surface area results in, the higher adsorption capacity of ZnOS+C[31].

On analyzing the zeta potential of ZnOS+C adsorbent at different pH, the isoelectric point, IEP was achieved at pH 2.8. This means that at pH lower than IEP, adsorbents have a positive charge on their surface, and while at pH higher than IEP, adsorbents have a negative charge on their surface. The charge on the adsorbent is a major driving force for the adsorption of dye on the adsorbent. ZnOS+C adsorbs negatively charged dye effectively at the lower pH and positively charged dye at higher pH. The zeta potential vs pH curve is plotted and shown in Figure S1.

## 3.2. Kinetic and isotherm study

### 3.2.1. Kinetic study

The batch study showed that on increasing the adsorbent dosages, the removal of dye increases and reaches the maximum at 22 mg of adsorbent. After that, a plateau was observed. Initially, the increase in the removal efficiency of dye is due to the increase in surface area and adsorbent sites. After 22 mg of adsorbent, a further increase in adsorbent dosage did not affect the dye removal

efficiency as the majority is already adsorbent at 22 mg of adsorbent. This result in the plateau formation. This trend is shown in Figure 4(a).

The pH variation of the solution affects the effective charge of adsorbate and controls the adsorption kinetic and mechanism involved. This affects the extent of the adsorption process. To study the pH dependence on removal efficiency of ZnOS+C, an equal amount of adsorbent was added to FG dye solutions of 25 mL, each having the same FG concentration, for equal time-interval maintained at different pH. Firstly, it was observed that the adsorbent effectively adsorbs the dye for a wide pH range from 2 to 9. Secondly, the optimum pH condition for maximum dye removal is 2-3. The removal efficiency of the adsorbent was high at low pH and decreased gradually with an increase in the pH, as shown in Figure 4(b). This obtained trend could be explained on the basis of isoelectronic point,  $pH_{zpc}$ . At lower pH, the adsorbent is positively charged and attracts negatively charged FG dye. While at higher pH, the adsorbent itself has a negative charge and repels the FG dye; hence removal efficiency of dye is lower at higher pH.

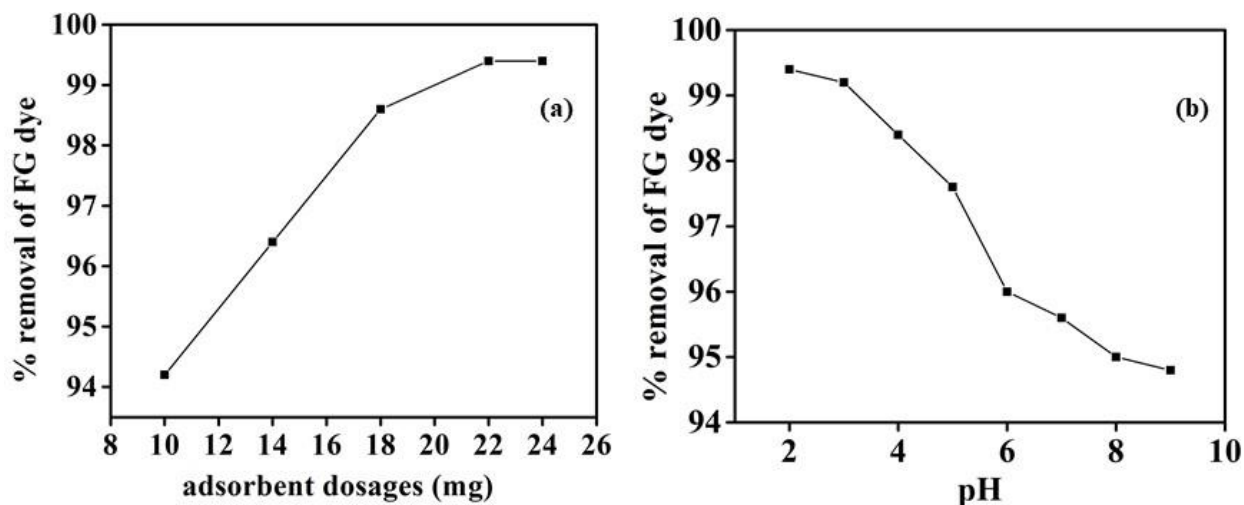


**Figure 4 FG dye adsorption on ZnOS+C in batch experiments: Volume of dye solution= 25 ml; (a) effect of adsorbent dosages and (b) effect of pH.**

The adsorption kinetic tests were performed to obtain the relationship between the dye adsorption and contact time. The adsorption of FG dye on ZnOS+C increases with an increase in the contact time, and adsorption equilibrium was obtained after 120 minutes. After that, any increase in the contact time did not affect the removal efficiency. A similar trend was reported by Sneha Chawla et al.[4] This can be explained as, at first, adsorbent sites were free and fully available for dye molecules, and hence adsorption takes place at a faster rate. But after some time, adsorbent sites were occupied by dye molecules, and finally, at equilibrium, the adsorbent was fully occupied, and no sites remained vacant. Hence, further contact time did not contribute to the increase in adsorption rate. This trend is shown in Figure S2 (a). Further, Figure S2 (b) shows that as the initial concentration of FG dye in the solution increases, FG dye removal efficiency decreases. A similar trend is reported by Sushmita Banerjee et al.[32], who used agricultural products as adsorbents to remove tartrazine dye.



Pseudo-first order, Pseudo-second order, and Intraparticle diffusion kinetic models were studied, and their data are fitted in the adsorption study. The linear equations of Pseudo-first order, Pseudo-second order, and Intraparticle diffusion kinetic model are respectively (3), (4), and (5).

$$\ln(q_e - q_t) = \ln q_e - K_1 t \quad (3)$$

$$\frac{t}{q_t} = \frac{1}{K_2 q_e^2} + \frac{t}{q_e} \quad (4)$$

$$q_t = C + K_3 t^{1/2} \quad (5)$$

Where  $q_e$  and  $q_t$  are the adsorption capacities at equilibrium and at time  $t$  in mg/g,  $K_1$ ,  $K_2$  and  $K_3$  are rate constant for Pseudo first order, Pseudo-second order, and intraparticle diffusion model, respectively.

Through the  $R^2$  value of each model, it was clear that the adsorption process best fits the intraparticle diffusion model of kinetics followed by pseudo-second order and then Pseudo-first order. The intraparticle diffusion model explains that the processes of diffusion of dye from wastewater to the adsorbent surface and adsorption of dye on the surface of the adsorbent are taking place simultaneously and have a significant effect on the adsorption rate. A similar type of trend is reported by Feng-Chin Wu et al.[33] for the removal of methylene blue dye from wastewater using activated carbon. Figure 5 and Table S1 show the result of the kinetic model fitting.

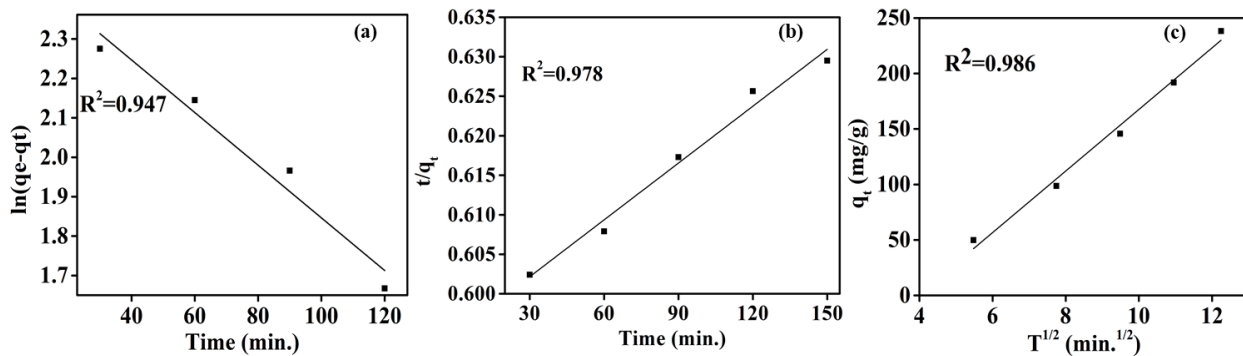


**Figure 5 FG dye adsorption on ZnOS+C in batch experiments: Volume of dye solution= 25 ml; adsorbent dosage= 22 mg; initial pH of dye solution= 2; contact time= 120 min; initial concentration of dye= 50 mg/g; (a) Pseudo 1st order; (b) Pseudo 2nd order and (c) Intraparticle diffusion kinetic model**

### 3.2.2. Isotherm test

To understand the adsorption mechanism and interaction between adsorbate and adsorbent, the data generated from batch studies fit into different isotherm models such as Langmuir, Freundlich, Temkin, and Dubinin- Radushkevich (D-R) isotherm. Each isotherm model has its significance and predicts the interaction between adsorbate and adsorbent and hence helps interpret the adsorption mechanism. Freundlich isotherm model predicts multilayered and heterogeneous adsorption.

The linear equation of the Freundlich isotherm model is;

$$\ln q_e = \ln K_f + \frac{1}{n} \ln C_f \quad (3)$$

Where  $q_e$  is equilibrium adsorption capacity in mg/g,  $K_f$ (mg/g) is Freundlich constant,  $n$  (unitless) is the adsorption intensity factor, and  $C_f$  is the final concentration of dye in solution.

While on the other hand, the Langmuir model goes for a homogeneously single-layered adsorption process, and its linear equation is;

$$\frac{C_f}{q_e} = \frac{1}{K_L Q_m} + \frac{C_f}{Q_m} \quad (4)$$

$$R_L = \frac{1}{1 + K_L C_e} \quad (5)$$

Where  $Q_m$  is maximum adsorption capacity in mg/g and  $K_L$  (L/g) is the Langmuir constant, which gives information about the energy of adsorption.  $R_L$  tells about the nature of adsorption, i.e.,  $R_L > 1$  means unfavorable adsorption,  $R_L < 1$  favorable adsorption, and  $R_L = 0$  irreversible adsorption.

Similarly, the D-R isotherm model predicts the interaction between adsorbent and adsorbate, i.e., physisorption or chemisorption. The linear equation of the D-R isothermal model is given by Equation 6,

$$\ln q_e = \ln q_m - K \epsilon^2 \quad (6)$$

Where  $K$  ( $\text{mol}^2/\text{KJ}^2$ ) is D-R constant and  $\epsilon$  is Polanyi potential and given by

$$\epsilon = RT \ln \left[ 1 + \frac{1}{C_e} \right] \quad (7)$$

$R$  (J/mol) is the gas constant, and  $T$  is the temperature in Kelvin.

$E = \frac{1}{\sqrt{2K}}$  is mean free energy in KJ/mol.

The Temkin isotherm model gives information about the heat of adsorption, which reduces linearly with coverage of adsorbent sites. The linear equation of the Temkin isotherm model is;

$$q_e = B \ln K_T + B \ln C_f \quad (8)$$

Where  $K_T$  is the Temkin constant in L/mg and  $B$  (J/mol) is related to the heat of adsorption.

The equations and data of different isotherms are put in Table 2, and the graph obtained is shown in Figure S3. On comparing the  $R^2$  value of different isotherms, the Freundlich model was found to be the best fit, followed by Langmuir, Temkin, and D-R. This explains the heterogeneously multilayered adsorption of FG dye on the surface of ZnOS+C. Also, the adsorption of FG dye on ZnOS+C surface follows the isotherm models in the order Freundlich > Langmuir > Temkin > D-R.

**Table 2 Different isotherm models**

<b>Freundlich isotherm</b>		<b>Temkin isotherm</b>		
$K_L$	83.09	$B$		48.35
$n$	2.42	$K_T$		7.24
$R^2$	0.993	$R^2$		0.927
<b>Langmuir isotherm</b>		<b>D-R isotherm</b>		
$q_m$	264.55	$q_m$		172.25
$K_L$	0.44	$K$		$9.8 \times 10^{-8}$
$R_L$	0.022	$E$		2.226
$R^2$	0.945	$R^2$		0.761

Also, the maximum adsorption capacity came out to be 238.28 mg of FG dye per gram of ZnOS+C. This adsorption capacity is compared with other reported adsorbents for FG dye and is shown in Table 3.

**Table 3 Comparison of different reported adsorbents for the removal of FG dye.**

<b>Adsorbents</b>	<b><math>q_e(\text{mg g}^{-1})</math></b>	<b>References</b>
<b>Activated carbon from <i>Gloriosasuperba</i></b>	51.02	[34]
<b>Activated carbon from <i>Alternariaraphani</i> Fungal biomass</b>	35.39	[34]

---

<b>Peanut hull</b>	15.60	[25]
<b>Tur dal husk</b>	100.39	[26]
<b>Tamarind husk</b>	101.58	[26]
<b>Bengal gram husk</b>	56.06	[26]
<b>Bottom Ash</b>	20.26	[27]
<b>De-oiled Soya</b>	5.31	[27]
<b>Montmorillonite Clay</b>	33.45	[28]
<b>Red Mud</b>	7.56	[35]
<b>Commercial Activated Carbon (AC)</b>	45.21	[36]
<b>CuS/ZnS-NCs-AC</b>	73.36	[36]
<b>ZnOS+C</b>	<b>238.28</b>	<b>Present work</b>

---

### 3.3. Thermodynamic study and mechanism involved

#### 3.3.1. Thermodynamic study

A thermodynamics study of adsorption of FG dye on ZnOS+C was performed to obtain the change in standard free energy ( $\Delta G^\circ$ ), standard entropy ( $\Delta S^\circ$ ), and standard enthalpy ( $\Delta H^\circ$ ). The batch experiments were performed at 3 different temperatures, 293 K, 303 K, and 313 K, and adsorption

data were obtained as shown in Table 4. The equilibrium constant (K) for the adsorption reaction was obtained by equation 9.

$$K_0 = \frac{c_0}{c_f} \quad (9)$$

The thermodynamic parameters were obtained with the help of equations 10 and 11.

$$\Delta G^\circ = -RT \ln K^\circ \quad (10)$$

$$\Delta G^\circ = \Delta H^\circ - T\Delta S^\circ \quad (11)$$

From equations 10 and 11, a linear equation 12 was derived as given below.

$$\ln K^\circ = \frac{\Delta S^\circ}{R} - \frac{\Delta H^\circ}{RT} \quad (12)$$

Using equation 12, Van't Hoff plot was drawn between  $\ln K^\circ$  against  $1/T$ , and values of  $\Delta H^\circ$  and  $\Delta S^\circ$  were derived from the slope and intercept, respectively. The Van't Hoff plot obtained by the thermodynamic study is shown in Figure S4.

The obtained negative value of  $\Delta H^\circ$  and  $\Delta S^\circ$  suggests that adsorption of FG dye on ZnOS+C is an exothermic process, and on the solid-liquid interface, entropy decreases, respectively. The negative value of  $\Delta G^\circ$  indicates the spontaneity of the adsorption process. Nada S. Al-Kadhi reported a similar trend of  $\Delta H^\circ$ ,  $\Delta S^\circ$ , and  $\Delta G^\circ$  for removal Lissamine Green B dye by micro-particle of wild plants[37].

**Table 4 Thermodynamic parameters for FG dye adsorption on ZnOS+C (Volume of dye solution= 25 ml; adsorbent dosage= 22 mg; initial pH of dye solution= 2; contact time= 120 min; initial concentration of dye= 100 mg/g)**

$\Delta H^\circ$ (KJ/mol)	$\Delta S^\circ$ (J/mol K)	$\Delta G^\circ$ (KJ/mol)
-65.09	-185.31	-10.57

### 3.3.2. Mechanism involved

The interaction between ZnOS+C and FG dye comprises many strong interactions such as electrostatic interaction between  $SO_3^-$  group of dye and Zn and C from the adsorbent, electrostatic interaction between  $N^+$  and O and S from the adsorbent, and Vander Waal interaction between the dye and adsorbent[30]. The combined effect of these interactions makes the ZnOS+C adsorbent highly potential for the uptake of FG dye from wastewater. The interaction between FG dye and ZnOS+C adsorbent is shown in Figure 6. The above explanation of electrostatic interaction can be explained through the results of the zeta potential study. At pH lower than an isoelectronic point, adsorbent surfaces have positively charged surfaces and have electrostatic interactions with negatively charged FG dye. This electrostatic interaction becomes weaker with an increase in pH. This is due to the negative surface charge on adsorbent with an increased pH.

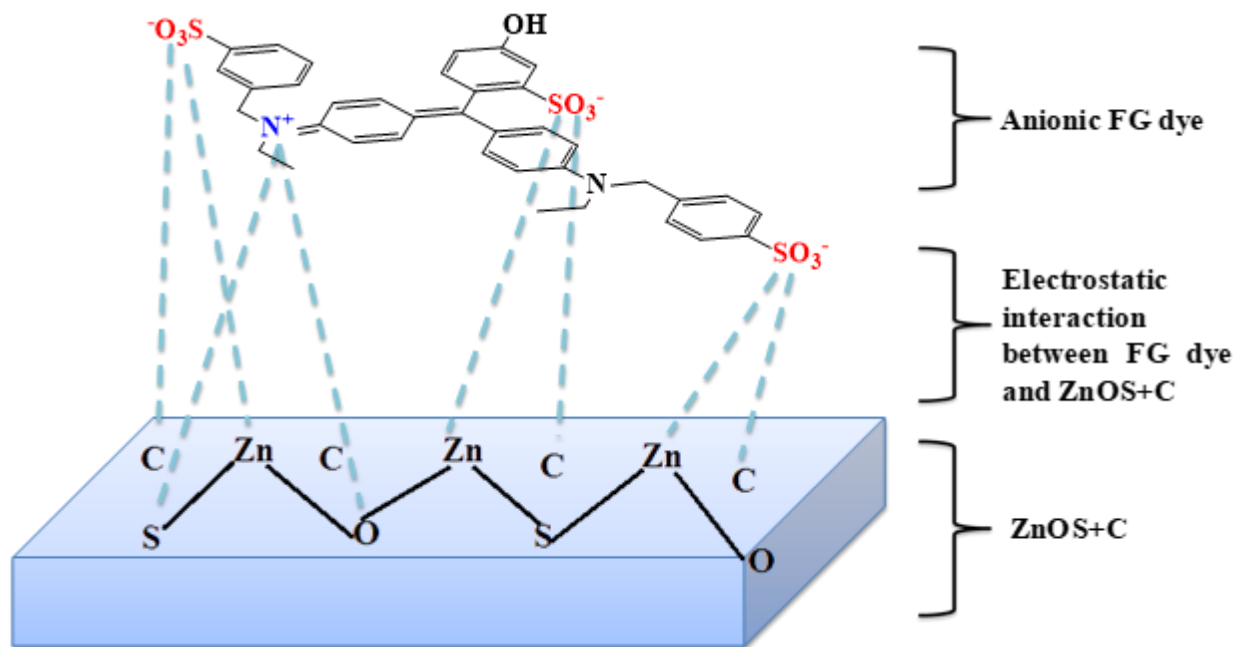


**Figure 6** Different types of interaction between FG dye and ZnOS+C adsorbent.

### 3.4. Anti-interference study

Different ions are present in wastewater along with organic dyes. These ions significantly affect the removal efficiency of adsorbent. So, to obtain the effects of coexisting ions present in dye wastewater, 0.1M 5 ml  $\text{Na}^+$ ,  $\text{Mg}^{2+}$ ,  $\text{Cl}^-$ ,  $\text{SO}_4^{2-}$ ,  $\text{PO}_3^{3-}$  ions solutions were introduced in dye solutions, and batch experiments were performed to obtain removal efficiency. The obtained results are shown in Figure 7. Anions influence the removal efficiency significantly and result in a decrease in removal efficiency. The same results are reported by Wang et al.[38], which suggests that anions compete with anionic FG dye and reduce the removal efficiency of dye on the ZnOS+C surface. In contrast, cations did not significantly affect the removal efficiency.

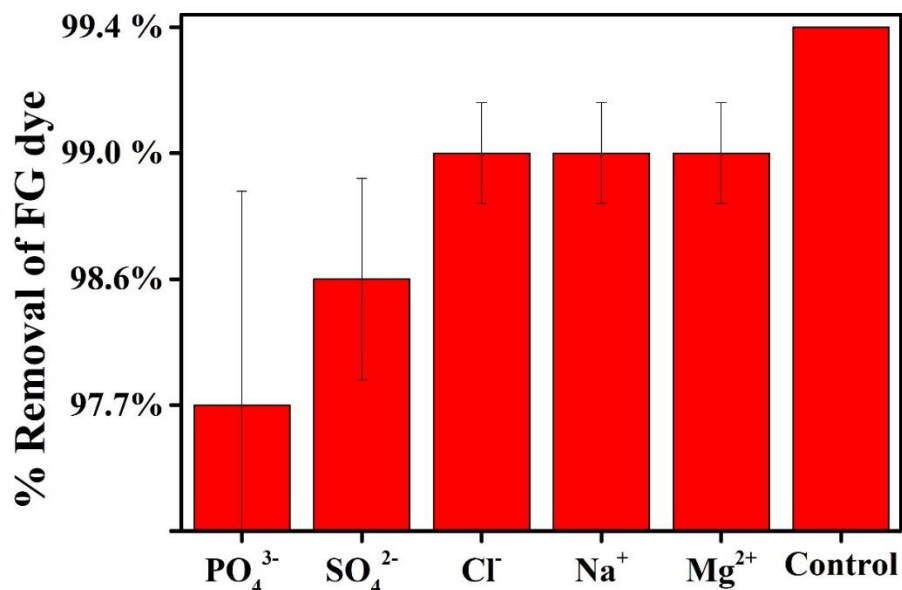


**Figure 7 Effects of coexistence of ions on the removal of FG dye.**

### **3.5. Novel ZnOS+C adsorbent for FG dye removal from real wastewater**

To validate the results obtained from the above studies and to ensure the effectiveness of adsorbent wastewater sample was collected from Such Exports Private Limited, Industrial Estate, Sonipat, Haryana, India. 0.11g of ZnOS+C adsorbent was added to 100 ml industrial wastewater at room temperature. The mixture was stirred for 120 minutes to obtain the best adsorption result. After the adsorption experiment, the mixture was centrifuged to separate the adsorbent from treated water, which was colorless, and then this colorless water was analyzed for FG dye concentration on a UV-VIS spectrophotometer. The concentration of FG dye in colorless water was found to be 0.03 mg/L, and this treated colorless water is found to be suitable for re-utilization by textile industries.

## **4. Conclusions**

ZnOS+C adsorbent was successfully synthesized through the wet chemical method. The adsorbent is found to be highly efficient for the removal of FG dye. It shows a high adsorption capacity of 238.28 mg/g, which is higher than the mostly reported adsorbents for FG dye. The high adsorption capacity of ZnOS+C is attributed to the chemical and electrostatic interaction between ZnOS+C and FG dye. These interactions result in the higher removal efficiency of the adsorbent. ZnOS+C also overcomes certain limitations of the conventional adsorbents, such as complex synthesis, low adsorption rate, low adsorption capacity, high adsorption time, high adsorbent dosages, and toxicity. It is eco-friendly, non-toxic, and highly efficient for uptake of FG dye with the adsorption efficiency of > 99%, which is very high compared to other reported adsorbents for the uptake of FG dye. The results from isotherm, kinetics, and thermodynamic studies support the proposed mechanism for dye removal.

Considering the high adsorption capacity of ZnOS+C adsorbent, it can be expected to show good removal efficiency for other contaminants, such as heavy metals, fluoride, and pesticides, which

will be a significant research direction in the future. The synthesized ZnOS+C believes in having a significant application for real wastewater treatment. This information is crucial for developing an advanced wastewater treatment system.

### **Credit authorship contribution statement**

**Sachin:** Conceptualization, Methodology, Investigation, Writing – original draft. **Biplob Kumar Pramanik:** Conceptualization, Writing – review & editing. **Harshit Gupta:** Writing – review & editing. **Shravan Kumar:** Editing. **Jai Shankar Tawale:** SEM and EDS explanation. **Kalpita Shah:** Writing – review & editing. **Nahar Singh:** Conceptualization, Project administration, Writing – review & editing.

### **Declaration of Competing Interest**

The authors declare that they have no known competing financial interests or personal relationships that could have appeared to influence the work reported in this paper.

### **Acknowledgments**

We thank the Director, CSIR-NPLI, for providing the required facilities and to the Council of Scientific and Industrial Research (CSIR) for offering research fellowships under the grant number 17/12/2017(ii)EU-V.

### **References**

- [1] S. Schulze, D. Zahn, R. Montes, R. Rodil, J.B. Quintana, T.P. Knepper, T. Reemtsma, U. Berger, Occurrence of emerging persistent and mobile organic contaminants in European water samples, *Water Res.* 153 (2019) 80–90. <https://doi.org/10.1016/j.watres.2019.01.008>.
- [2] S. Kim, F. Gholamirad, B. Shin, N. Taheri-Qazvini, J. Cho, M. Yu, C.M. Park, J. Heo, Y. Yoon, Application of a  $Ti_3C_2T_x$  MXene-Coated Membrane for Removal of Selected Natural Organic Matter and Pharmaceuticals, *ACS EST Water.* 1 (2021) 2164–2173. <https://doi.org/10.1021/acsestwater.1c00242>.
- [3] Jaishree, Sachin, Natural Products and By-Products as a Cost-Effective Adsorbent for Cr (VI) Removal from Water Sources: A Review, *Austin Environ. Sci.* 7 (2022). <https://doi.org/10.26420/austinenvirosci.2022.1074>.
- [4] S. Chawla, H. Uppal, M. Yadav, N. Bahadur, N. Singh, Zinc peroxide nanomaterial as an adsorbent for removal of Congo red dye from waste water, *Ecotoxicol. Environ. Saf.* 135 (2017) 68–74. <https://doi.org/10.1016/j.ecoenv.2016.09.017>.
- [5] J.C. Baum, M. Feng, B. Guo, C.-H. Huang, V.K. Sharma, Generation of Iron(IV) in the Oxidation of Amines by Ferrate(VI): Theoretical Insight and Implications in Oxidizing Pharmaceuticals, *ACS EST Water.* 1 (2021) 1932–1940. <https://doi.org/10.1021/acsestwater.1c00156>.
- [6] A. Othmani, S. Magdouli, P. Senthil Kumar, A. Kapoor, P.V. Chellam, Ö. Gökkuş, Agricultural waste materials for adsorptive removal of phenols, chromium (VI) and cadmium (II) from wastewater: A review, *Environ. Res.* 204 (2022) 111916. <https://doi.org/10.1016/j.envres.2021.111916>.



- [7] P.J. Van den Brink, J.V. Tarazona, K.R. Solomon, T. Knacker, N.W. Van den Brink, T.C.M. Brock, J.P. (Hans) Hoogland, The use of terrestrial and aquatic microcosms and mesocosms for the ecological risk assessment of veterinary medicinal products, *Environ. Toxicol. Chem.* 24 (2005) 820–829. <https://doi.org/10.1897/04-268R.1>.
- [8] Sachin, D. Joishar, N.P. Singh, E. Varathan, N. Singh, Sodium Docusate Surface-Modified Dispersible and Powder Zinc Peroxide Formulation: An Adsorbent for the Effective and Fast Removal of Crystal Violet Dye, an Emerging Wastewater Contaminant, *ACS Omega.* 6 (2021) 22570–22577. <https://doi.org/10.1021/acsomega.1c02324>.
- [9] M.M. Hassan, C.M. Carr, A critical review on recent advancements of the removal of reactive dyes from dyehouse effluent by ion-exchange adsorbents, *Chemosphere.* 209 (2018) 201–219. <https://doi.org/10.1016/j.chemosphere.2018.06.043>.
- [10] C. Lubinski, Global Trade and Indian Politics: The German Dye Business in India before 1947, *Bus. Hist. Rev.* 89 (2015) 503–530. <https://doi.org/10.1017/S0007680515000707>.
- [11] H. Lachheb, E. Puzenat, A. Houas, M. Ksibi, E. Elaloui, C. Guillard, J.-M. Herrmann, Photocatalytic degradation of various types of dyes (Alizarin S, Crocein Orange G, Methyl Red, Congo Red, Methylene Blue) in water by UV-irradiated titania, *Appl. Catal. B Environ.* 39 (2002) 75–90. [https://doi.org/10.1016/S0926-3373\(02\)00078-4](https://doi.org/10.1016/S0926-3373(02)00078-4).
- [12] R. López Cisneros, A. Gutarra Espinoza, M.I. Litter, Photodegradation of an azo dye of the textile industry, *Chemosphere.* 48 (2002) 393–399. [https://doi.org/10.1016/S0045-6535\(02\)00117-0](https://doi.org/10.1016/S0045-6535(02)00117-0).
- [13] U.N. Wiesmann, S. DiDonato, N.N. Herschkowitz, Effect of chloroquine on cultured fibroblasts: release of lysosomal hydrolases and inhibition of their uptake, *Biochem. Biophys. Res. Commun.* 66 (1975) 1338–1343. [https://doi.org/10.1016/0006-291x\(75\)90506-9](https://doi.org/10.1016/0006-291x(75)90506-9).
- [14] G. Sharma, A. Kumar, S. Sharma, S.I. Al-Saeedi, G.M. Al-Senani, A. Nafady, T. Ahamad, Mu. Naushad, F.J. Stadler, Fabrication of oxidized graphite supported La<sub>2</sub>O<sub>3</sub>/ZrO<sub>2</sub> nanocomposite for the photoremediation of toxic fast green dye, *J. Mol. Liq.* 277 (2019) 738–748. <https://doi.org/10.1016/j.molliq.2018.12.126>.
- [15] C.A. Murray, S.A. Parsons, Advanced oxidation processes: flowsheet options for bulk natural organic matter removal, *Water Supply.* 4 (2004) 113–119. <https://doi.org/10.2166/ws.2004.0068>.
- [16] S. Kim, K.H. Chu, Y.A.J. Al-Hamadani, C.M. Park, M. Jang, D.-H. Kim, M. Yu, J. Heo, Y. Yoon, Removal of contaminants of emerging concern by membranes in water and wastewater: A review, *Chem. Eng. J.* 335 (2018) 896–914. <https://doi.org/10.1016/j.cej.2017.11.044>.
- [17] C.A. Basha, K. Ramanathan, R. Rajkumar, M. Mahalakshmi, P.S. Kumar, Management of Chromium Plating Rinsewater Using Electrochemical Ion Exchange, *Ind. Eng. Chem. Res.* 47 (2008) 2279–2286. <https://doi.org/10.1021/ie070163x>.
- [18] M.S. Oncel, A. Muhcu, E. Demirbas, M. Kobya, A comparative study of chemical precipitation and electrocoagulation for treatment of coal acid drainage wastewater, *J. Environ. Chem. Eng.* 1 (2013) 989–995. <https://doi.org/10.1016/j.jece.2013.08.008>.
- [19] R. Costa, P. Dugo, L. Mondello, Sampling and Sample Preparation Techniques for the Determination of the Volatile Components of Milk and Dairy Products, in: *Compr. Sampl. Sample Prep.*, Elsevier, 2012: pp. 43–59. <https://doi.org/10.1016/B978-0-12-381373-2.00127-7>.

- [20] B. Pilat, Practice of water desalination by electrodialysis, *Desalination*. 139 (2001) 385–392. [https://doi.org/10.1016/S0011-9164\(01\)00338-1](https://doi.org/10.1016/S0011-9164(01)00338-1).
- [21] A. Yadav, N. Bagotia, A.K. Sharma, S. Kumar, Advances in decontamination of wastewater using biomass-based composites: A critical review, *Sci. Total Environ.* 784 (2021) 147108. <https://doi.org/10.1016/j.scitotenv.2021.147108>.
- [22] A. Othmani, S. Magdoui, P. Senthil Kumar, A. Kapoor, P.V. Chellam, Ö. Gökkuş, Agricultural waste materials for adsorptive removal of phenols, chromium (VI) and cadmium (II) from wastewater: A review, *Environ. Res.* 204 (2022) 111916. <https://doi.org/10.1016/j.envres.2021.111916>.
- [23] Y. Zhou, J. Lu, Y. Zhou, Y. Liu, Recent advances for dyes removal using novel adsorbents: A review, *Environ. Pollut.* 252 (2019) 352–365. <https://doi.org/10.1016/j.envpol.2019.05.072>.
- [24] N.C. Corda, M.S. Kini, A Review on Adsorption of Cationic Dyes using Activated Carbon, *MATEC Web Conf.* 144 (2018) 02022. <https://doi.org/10.1051/mateconf/201814402022>.
- [25] R. Gong, Y. Sun, J. Chen, H. Liu, C. Yang, Effect of chemical modification on dye adsorption capacity of peanut hull, *Dyes Pigments.* 67 (2005) 175–181. <https://doi.org/10.1016/j.dyepig.2004.12.003>.
- [26] D. Kanamadi, N. Ahalya, T.V. Ramachandra, Low cost biosorbents for dye removal, (2006).
- [27] A. Mittal, D. Kaur, J. Mittal, Batch and bulk removal of a triarylmethane dye, Fast Green FCF, from wastewater by adsorption over waste materials, *J. Hazard. Mater.* 163 (2009) 568–577. <https://doi.org/10.1016/j.jhazmat.2008.07.005>.
- [28] T. Hajira, H. Uzma, S. Muhammad, J. Qazi, Batch adsorption technique for the removal of malachite green and fast green dyes by using montmorillonite clay as adsorbent, *Afr. J. Biotechnol.* 9 (2010) 8206–8214. <https://doi.org/10.5897/AJB10.911>.
- [29] V.K. Gupta, Suhas, I. Ali, V.K. Saini, Removal of Rhodamine B, Fast Green, and Methylene Blue from Wastewater Using Red Mud, an Aluminum Industry Waste, *Ind. Eng. Chem. Res.* 43 (2004) 1740–1747. <https://doi.org/10.1021/ie034218g>.
- [30] H. Uppal, S. Chawla, A.G. Joshi, D. Haranath, N. Vijayan, N. Singh, Facile chemical synthesis and novel application of zinc oxysulfide nanomaterial for instant and superior adsorption of arsenic from water, *J. Clean. Prod.* 208 (2019) 458–469. <https://doi.org/10.1016/j.jclepro.2018.10.023>.
- [31] M. Anjum, R. Miandad, M. Waqas, F. Gehany, M.A. Barakat, Remediation of wastewater using various nano-materials, *Arab. J. Chem.* 12 (2019) 4897–4919. <https://doi.org/10.1016/j.arabjc.2016.10.004>.
- [32] S. Banerjee, M.C. Chattopadhyaya, Adsorption characteristics for the removal of a toxic dye, tartrazine from aqueous solutions by a low cost agricultural by-product, *Arab. J. Chem.* 10 (2017) S1629–S1638. <https://doi.org/10.1016/j.arabjc.2013.06.005>.
- [33] F.-C. Wu, R.-L. Tseng, R.-S. Juang, Initial behavior of intraparticle diffusion model used in the description of adsorption kinetics, *Chem. Eng. J.* 153 (2009) 1–8. <https://doi.org/10.1016/j.cej.2009.04.042>.
- [34] S. Ramalakshmi, K. Muthucheli, K. Swaminatha, Comparative Studies on Removal of Fast Green Dye from Aqueous Solutions by Activated Carbon Prepared from *Gloriosa superba* Waste and *Alternaria raphani* Fungal Biomass, *J. Environ. Sci. Technol.* 5 (2012) 222–231. <https://doi.org/10.3923/jest.2012.222.231>.

- [35] V.K. Gupta, Suhas, I. Ali, V.K. Saini, Removal of Rhodamine B, Fast Green, and Methylene Blue from Wastewater Using Red Mud, an Aluminum Industry Waste, *Ind. Eng. Chem. Res.* 43 (2004) 1740–1747. <https://doi.org/10.1021/ie034218g>.
- [36] J. Pooralhossini, M. Ghaedi, M.A. Zanjanchi, A. Asfaram, Ultrasonically assisted removal of Congo Red, Phloxine B and Fast green FCF in ternary mixture using novel nanocomposite following their simultaneous analysis by derivative spectrophotometry, *Ultrason. Sonochem.* 37 (2017) 452–463. <https://doi.org/10.1016/j.ultsonch.2017.01.038>.
- [37] N.S. Al-Kadhi, The kinetic and thermodynamic study of the adsorption Lissamine Green B dye by micro-particle of wild plants from aqueous solutions, *Egypt. J. Aquat. Res.* 45 (2019) 231–238. <https://doi.org/10.1016/j.ejar.2019.05.004>.
- [38] H. Wang, X. Yuan, G. Zeng, L. Leng, X. Peng, K. Liao, L. Peng, Z. Xiao, Removal of malachite green dye from wastewater by different organic acid-modified natural adsorbent: kinetics, equilibriums, mechanisms, practical application, and disposal of dye-loaded adsorbent, *Environ. Sci. Pollut. Res.* 21 (2014) 11552–11564. <https://doi.org/10.1007/s11356-014-3025-2>.